August 27-31, 2023
FLORENCE - ITALY
16th International Conference on Wind Engineering
ICWE 16

Wind loading features of rooftop solar arrays of tall buildings with applications to roof zoning

H.Y. Peng[1], S.F. Dai[1], H.J. Liu[1]

[1] *School of Civil and Environmental Engineering, Harbin Institute of Technology, Shenzhen, China, penghuayi@hit.edu.cn*

SUMMARY:
An experimental study was carried out to investigate the wind loads on roof-mounted solar arrays. The effects of panel location, tilt angle β, and building height H were studied. The largest most critical module force coefficients among all modules and wind angles decreased as building height increased. This was attributed to that the approaching flows tended to separate from roof edges rather than building sides of low-rise buildings. The most critical module force coefficients varied greatly with roof locations. To balance the design costs and structural safety, the roof zoning for wind loads on solar arrays was examined by the k-means method. Roofs could be divided into three zones, i.e., corner, edge, and interior zones. Besides, the mathematical models of design loads for building heights at various roof zones were analysed considering the results of roof zoning. Peak loads at corner zones tended to be underestimated by the existing relevant design codes because high turbulence intensities induced by solar arrays and roofs were not respected. The developed models can provide recommendations for design wind loads on solar arrays at various roof zones.

Keywords: wind loads, rooftop solar arrays, roof zoning, wind tunnel test, k-means

1. GENERAL INSTRUCTIONS

Rooftops solar arrays have become more and more popular as no additional land is required (Chu and Tsao, 2018). Wind load is the major concern in designing rooftop solar arrays for these systems, and plays a significant role in the installation. The literature investigated wind loads on solar arrays of low-rise buildings (Banks,2013; Naeiji et al., 2017). Hence, wind loads on solar arrays mounted on roofs of different heights need further investigations. Moreover, the zoning strategy for wind loads on rooftop solar arrays is barely observed in the literature. Nevertheless, the literature reports that the mean and peak wind loads on rooftop solar arrays fluctuate greatly with roof locations (Stathopoulos et al., 2014; Dai et al., 2022). Considering the balance of design costs and structural safety, roof zoning is required to properly determine the design wind loads on rooftop solar arrays.

2. EXPERIMENTAL SETUP

2.1. Details of building and solar panel models

The geometric scale of buildings and solar arrays was 1:100. The width and depth of four different buildings were identical, i.e., 24 m. The roof heights were 24 m, 48 m, 72 m, and 96 m at full scale. Fig. 1 shows the test models and pressure measurement system. s and d referred to the setback distance and the spacing between adjacent solar arrays, respectively. The layout of solar arrays on the roof is represented in Fig. 1(c). The clearance between the lower ends of solar arrays and the roof was fixed at 0.5 m at full scale. The ESP-64HD pressure scanner was utilized for pressure measurement.

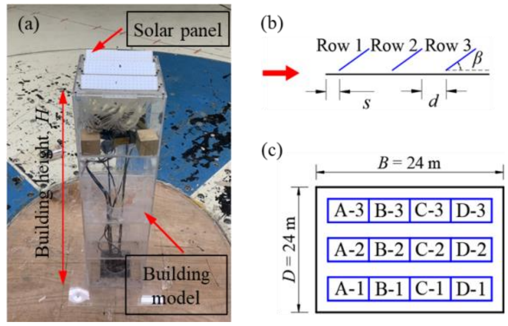

Figure 1. Experimental models: (a) test models and measurement system in the wind tunnel, (b) Schematic of solar arrays at side view, and (c) layout of solar arrays on the roof.

2.2. Data treatment

The module force coefficient C_{fm} is calculated as follows:

$$C_{fm} = \sum_{i=1}^{n} A_i C_{pn}(i) / \sum_{i=1}^{n} A_i \tag{1}$$

where n = 3 for a module, C_{pn} denotes tap pressure coefficient, and A_i represents area of a module.

3. RESULTS AND DISCUSSIONS

Fig. 2 shows the most critical mean and negative peak module force coefficients C_{fm} among all wind angles θ at each module. $\overline{C}_{fm}$ and $\breve{C}_{fm}$ referred to the mean and negative peak C_{fm}, respectively. The modules at roof corners were subjected to the largest wind loads, followed by modules at roof edges, while modules at roof centers experienced the smallest wind loads. Large loads at roof corners can be attributed to strong conical vortices at oblique θ (Wang et al., 2020).

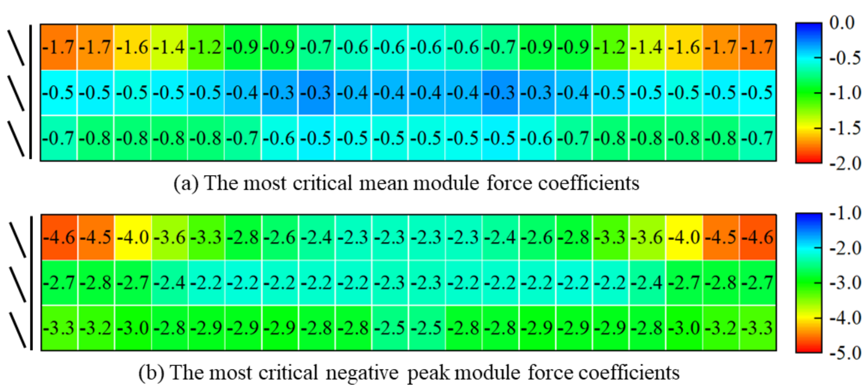

Figure 2. Distribution of the most critical module force coefficients: (a) mean, and (b) negative peak.

To consider the balance between design costs and structural safety, roof zoning for wind loads on solar arrays needed to be analyzed. Wind loads from tests provided data for roof clustering by the *k*-means algorithm. The purpose of *k*-means clustering approach was to group observations. The flow chart of *k*-means algorithm for roof zoning of solar arrays is depicted in Fig. 3. $\breve{C}_{fm,m\text{-}n}$ and

B in Fig. 3 denote the largest $\breve{C}_{fm}$ among all wind angles on each module and building width, respectively.

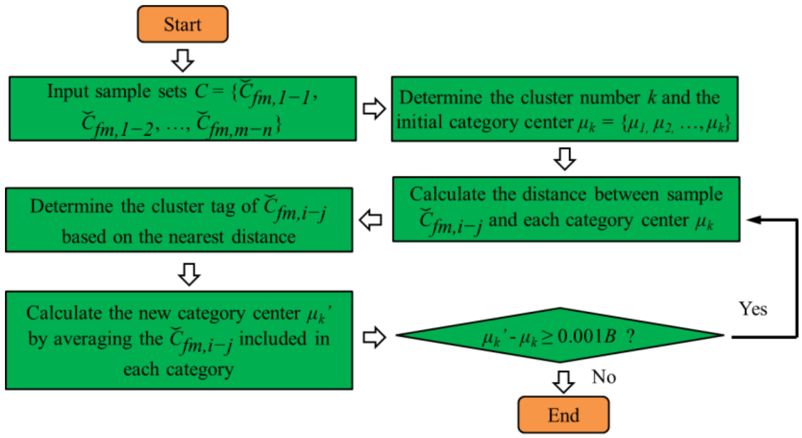

Figure 3. Flow chart of the *k*-means algorithm for roof zoning of solar arrays.

Fig. 4 shows the roof zoning results of wind loads based on the *k*-means clustering approach. Roofs could be divided into three zones, i.e., corner, edge, and interior zones. The edge zones covered the largest area of the roof, followed the corner zone, while the interior zone was the smallest. The zoning scheme can provide recommendations for the wind load design of rooftop solar arrays.

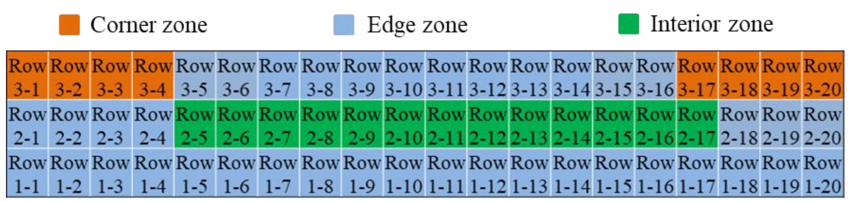

Figure 4. Roof zoning of solar arrays based on the *k*-means algorithm.

Fig. 5 presents the largest most critical $\overline{C}_{fm}$ and $\breve{C}_{fm}$ at the corner zone with a building height of *H*. The largest most critical $\overline{C}_{fm}$ and $\breve{C}_{fm}$ decreased linearly as *H* increased. Furthermore, the largest most critical $\breve{C}_{fm}$ at roof corner were noticeably underestimated by JIS C 8955 (2017) because high turbulence intensities induced by solar arrays and roofs were not considered.

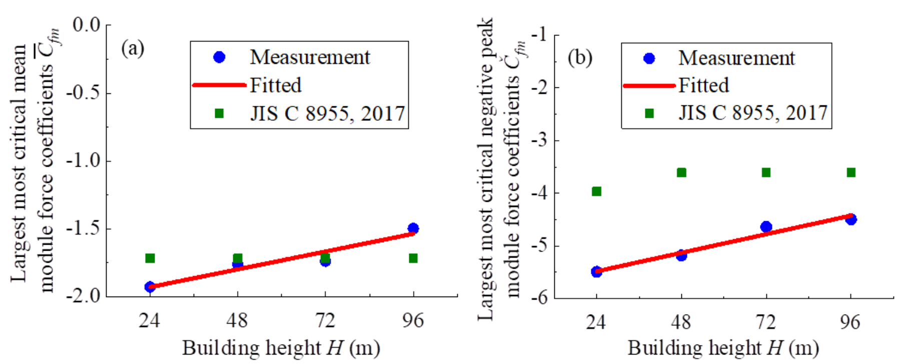

Figure 5. Effect of *H* on the largest most critical $\overline{C}_{fm}$ and $\breve{C}_{fm}$ at corner zone: (a) $\overline{C}_{fm}$ and (b) $\breve{C}_{fm}$.

The largest most critical $\overline{C}_{fm}$ and $\breve{C}_{fm}$ in each roof zone at H can be predicted by Eqs. (2)-(4).

$$\text{Corner zone}\begin{cases}\overline{C}_{fm} = 0.0055H - 2.062 \text{ (24 m} \le H \le \text{96 m)} \\ \breve{C}_{fm} = 0.0147H - 5.837 \text{ (24 m} \le H \le \text{96 m)}\end{cases} \tag{2}$$

$$\text{Edge zone}\begin{cases}\overline{C}_{fm} = 0.0025H - 1.004 \text{ (24 m} \le H \le \text{96 m)} \\ \breve{C}_{fm} = 0.0067H - 3.630 \text{ (24 m} \le H \le \text{96 m)}\end{cases} \tag{3}$$

$$\text{Interior zone}\begin{cases}\overline{C}_{fm} = 0.0012H - 0.518 \text{ (24 m} \le H \le \text{96 m)} \\ \breve{C}_{fm} = 0.0067H - 2.838 \text{ (24 m} \le H \le \text{96 m)}\end{cases} \tag{4}$$

4. CONCLUSIONS

In this study, the effect of building height H on wind loads on roof-mounted solar arrays was investigated through wind tunnel tests. The largest most critical mean and negative peak module force coefficients decreased as H increased. The most critical $\overline{C}_{fm}$ and $\breve{C}_{fm}$ among all θ varied greatly with panel locations. To consider the balance between design costs and structural safety, the roof zoning for wind loads was examined by using the k-means approach. The roof could be clustered into three categories, i.e., corner, edge, and interior zones. The largest most critical $\breve{C}_{fm}$ on modules at the corner zone tended to be underestimated according to JIS C 8955 as high turbulence induced by building and solar arrays was not considered. The mathematical models of wind loads provided recommendations for the design of solar arrays and their supporting structures at various H.

ACKNOWLEDGEMENTS

This work was supported by Shenzhen Science and Technology Innovation Committee (Grant No. GXWD20201230155427003-20200824100128002), National Natural Science Foundation of China (NSFC) (Grant No. 51978221), and Characteristic and Innovation Projects of Universities in Guangdong Province (Grant No. 2021KTSCX367).

REFERENCES

Banks, D., 2013. The role of corner vortices in dictating peak wind loads on tilted flat solar panels mounted on large, flat roofs. Journal of Wind Engineering and Industrial Aerodynamics 123, 192–201.

Chu, C. R. and Tsao, S. J., 2018. Aerodynamic loading of solar trackers on flat-roofed buildings. Journal of Wind Engineering and Industrial Aerodynamics 175, 202–212.

Dai S. F., Liu H. J., Yang J. H., and Peng H. Y., 2022. Wind loads on roof-mounted isolated solar panels of tall buildings through wind tunnel testing. Solar Energy 231, 607–622.

JIS C 8955, 2017. Design Guide on Structures for Photovoltaic Array, Tokyo: Japanese Industrial Standards Committee.

Naeiji A., Raji F., and Zisis I., 2017. Wind loads on residential scale rooftop photovoltaic panels. Journal of Wind Engineering and Industrial Aerodynamics 168, 228–246.

Stathopoulos T., Zisis I., and Xypnitou E., 2014. Local and overall wind pressure and force coefficients for solar panels. Journal of Wind Engineering and Industrial Aerodynamics 125, 195–206.

Wang J. X., Yang Q., Phuc P. V., and Tamura Y., 2020. Characteristics of conical vortices and their effects on wind pressures on flat-roof-mounted solar arrays by LES. Journal of Wind Engineering and Industrial Aerodynamics 200, 104146.